Kinetic Isotope Effects in Complex Reaction Networks: Formic Acid Electro-Oxidation

ARTICLE *in* CHEMPHYSCHEM · FEBRUARY 2007

Impact Factor: 3.42 · DOI: 10.1002/cphc.200600520 · Source: PubMed

CHEMPHYSCHEM

DOI: 10.1002/cphc.200600520

Kinetic Isotope Effects in Complex Reaction Networks: Formic Acid Electro-Oxidation

Yan-Xia Chen,* Martin Heinen, Zenonas Jusys, and Rolf Jürgen Behm*[a]

The determination of kinetic isotope effects (KIEs) for different reaction pathways and steps in a complex reaction network, where KIEs may affect the overall reaction in various different ways including dominant and minority pathways or the buildup of a reaction-inhibiting adlayer, is demonstrated for formic acid electro-oxidation on a Pt film electrode by quantitative electrochemical in situ IR spectroscopic measurements under controlled mass-transport conditions. The ability to separate effects resulting from different contributions—which is not possible using purely electrochemical kinetic measurements—allows conclusions on the nature of the rate-limiting steps and their transition state in the individual reaction pathways. The potential-independent values of ≈1.9 for the KIE of formic acid dehydration (CO_{ad} formation) in the indirect pathway and ≈3 for the CO_{ad} coverage-normalized KIE of formic acid oxidation to CO_2 (direct pathway) indicate that 1) C–H bond breaking is rate-limiting in both reaction steps, 2) the transition states for these reactions are different, and 3) the configurations of the transition states involve rather strong bonds to the transferred D/H species, either in the initial or in the final state, for the direct pathway and—even more pronounced—for formic acid dehydration (CO_{ad} formation).

Introduction

Kinetic isotope effects (KIEs) have long been used to unravel mechanistic details in chemical and electrochemical reactions.[1–6] In many cases, however, the information gained from reaction kinetic measurements cannot be attributed to a specific reaction pathway and/or to a specific rate-limiting step but it rather results from a complex combination of different reaction pathways and reaction steps, which contribute to the total reaction and the measured reaction rates. Herein, we demonstrate how the KIE of specific reaction pathways can be determined by combined kinetic and in situ IR spectroscopic measurements and how the measured effective KIE can be influenced by different contributions, which include the genuine KIEs in the different reaction pathways and contributions from the buildup of reaction-inhibiting adlayers, whose buildup rate and steady-state coverages may differ for different isotopomers. This is demonstrated for the electro-oxidation of formic acid on a Pt film electrode by characterizing the reaction and adsorbed reaction products/intermediates by means of electrochemical in situ IR spectroscopy measurements in an attenuated total reflection (ATR) configuration under controlled mass-transport conditions.[7]

Based on electrochemical,[8–10] in situ IR spectroscopic,[11–13] and differential electrochemical mass spectrometry (DEMS) measurements, using ^{13}C-labeled formic acid,[14] a so-called *dual pathway* mechanism has already been established for this reaction, which involves the following formal reaction pathways [Eqs. (1) and (2)]:

$$HCOOH \rightarrow CO_2 + 2\,H^+ + 2\,e^- \quad (1)$$

$$HCOOH \rightarrow CO_{ad} + H_2O \text{ and} \quad (2a)$$

$$H_2O \rightarrow OH_{ad} + H^+ + e^- \text{ and} \quad (2b)$$

$$CO_{ad} + OH_{ad} \rightarrow CO_2 + H^+ + e^- \quad (2c)$$

The first pathway [Eq. (1)] was denoted as a *direct pathway*, while the other set of reactions [Eqs. (2a)–(2c)] was described as the *indirect pathway*. Later, it was proposed that the *direct pathway* proceeds via formation and oxidation of bridge-bonded, adsorbed formate species.[15–19] From a quantitative evaluation of the intensities of the adsorbed-formate IR signals recorded under reaction conditions and their temporal evolution upon electrolyte exchange (from supporting electrolyte to formic-acid-containing solution and back), Chen et al.[7,20] found that under standard reaction conditions (up to 0.75 V, at formic acid concentrations ≥0.1 M), this pathway is a minority pathway, which means that there must be a third pathway that proceeds via direct reaction, without an IR-detectable adsorbed intermediate, and which under those conditions is dominant. Consequently, these authors described the latter pathway as the *direct pathway* and the other one, which pro-

[a] *Prof. Y.-X. Chen,[+] M. Heinen, Dr. Z. Jusys, Prof. R. J. Behm*
Department of Surface Chemistry and Catalysis
University of Ulm, 89069 Ulm (Germany)
Fax:(+49) 731-5025452
E-mail: juergen.behm@uni-ulm.de

[+] *Current address:*
Hefei National Laboratory for Physical Sciences at Microscale
Department of Chemical Physics
University of Science and Technology of China
E-mail: yachen@ustc.edu.cn

ceeds via the formation and oxidation of adsorbed bridge-bonded formates, as the *formate pathway*. Finally, there seems to be general agreement that under most reaction conditions, the *indirect pathway* contributes very little to the total reaction process, usually only about one percent or less.[7,18–20] Accordingly, CO_{ad} mainly acts as a catalyst poison rather than as a reaction intermediate. Despite these numerous proposals on the reaction mechanism, details on the molecular-scale mechanism and on the nature of the transition states in the different pathways are largely unknown. These are the topics of the present study, which aims at deriving mechanistic information by determining pathway-specific KIEs. This objective was approached by simultaneous electrochemical and quantitative in situ IR spectroscopic flow-cell experiments, where we followed the buildup of the CO adlayer and the evolution of the Faradaic current upon interaction of a clean, CO_{ad}-free Pt film electrode with a deuterated (DCOOH) or unlabelled (HCOOH) formic acid solution at different adsorption potentials under controlled flow conditions.

To the best of our knowledge, previous mechanistic investigations of KIEs in C1 molecule oxidation reactions relied, with few exceptions,[21,22] on electrochemical measurements, mostly cyclic voltammetry, comparing the total Faradaic current during the potential scan.[2,4–6] In those cases, the differences in adlayer composition and coverages during the reaction and possible contributions from different reaction pathways for the different isotopomers render an accurate evaluation of reaction-specific KIE factors impossible. The experimental procedure applied here is applicable for mechanistic studies involving a wide range of electrochemical or chemical surface reactions, and thus, it is of more general interest than just the present type of electrocatalytic reaction.

Experimental Section

The experiments were performed in a thin-layer spectroelectrochemical flow cell, which allows in situ IR measurements in an ATR configuration under controlled mass-transport conditions, as described in detail elsewhere.[7,23] The cell volume was $\approx$150 μL, the flow rate applied in the experiment was about 100 $\mu L\,s^{-1}$. The Pt working electrode (exposed area ca. 1 cm^2, surface roughness factor ca. 5) was prepared by electroless Pt deposition on a Si prism following the procedure described in ref. [17]; two Pt foils and a reversible hydrogen electrode (RHE) served as counter and reference electrodes. The electrolyte solutions were prepared using formic acid (HCOOH, Merck, p.a. grade; DCOOH, Sigma–Aldrich, 95% in water), suprapure H_2SO_4 (Merck), and Millipore water (18.2 $M\Omega\,cm^{-1}$). They were deaerated with high-purity Ar gas (N6.0) for 20 min before each experiment. All experiments were performed at room temperature. IR spectra were measured using a BioRad FTS-6000 spectrometer, equipped with a mercury–cadmium–telluride (MCT) detector at a resolution of 4 cm^{-1}, co-adding five interferograms for each spectrum (ca. 1 s per spectrum). The intensities are given as absorbance, defined by $\log(R_0/R)$, where R_0 and R are the reflectance of the reference and sample spectrum, respectively. The reference spectrum was recorded at the same potential in pure base electrolyte. This data processing results in spectra in which the peaks pointing up reflect an increased absorption, and the peaks pointing down reflect a loss of absorption, relative to the reference spectrum.

Results and Discussion

Figure 1 shows Faradaic current density transients recorded upon changing from a pure base electrolyte to a 0.02 M formic acid-containing solution at different potentials [from 0.1 to 0.5 V, a) HCOOH, b) DCOOH]. These transients largely resemble previous data,[7] with a steep initial increase and, after passing through a sharp maximum, an initially fast and then increasingly slower decay. Steady-state conditions are reached after 300 s only at lower potentials, while for $E \geq 0.4$ V slow changes in the reaction occur also at later times (see below). Furthermore, the transients reveal a clear increase in the current density with the electrode potential for both the HCOOH and DCOOH oxidation. At the same potential, the current densities observed for HCOOH are higher than those observed for DCOOH.

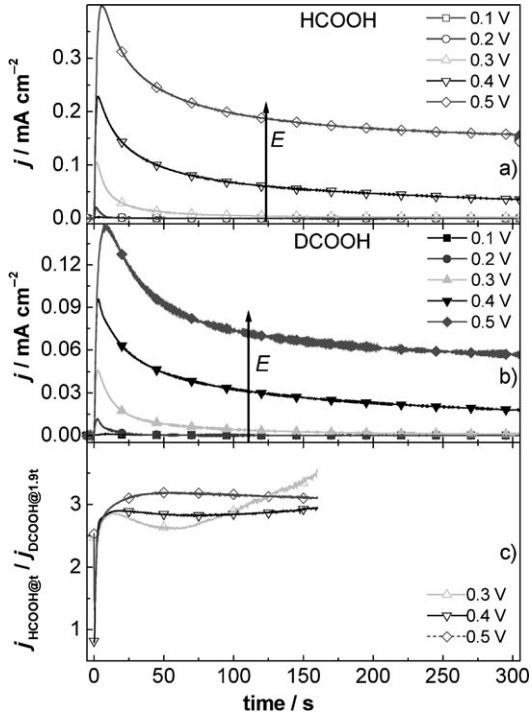

Figure 1. Current-density transients recorded at different potentials (0.1–0.5 V) on a Pt film electrode after changing from a pure 0.5 M H_2SO_4 base electrolyte to 0.02 M HCOOH (a) and DCOOH (b) containing 0.5 M H_2SO_4 solutions. c) Temporal evolution of the measured effective KIEs at different electrode potentials, as derived from the Faradaic currents for HCOOH and the time-normalized current for the DCOOH oxidation at different potentials.

Figure 2 shows sequences of IR spectra recorded upon electrolyte exchange (Figures 2a and 2c: HCOOH; Figures 2b and 2d: DCOOH) at 0.1 (Figures 2a and 2b) and 0.4 V (Figures 2c and 2d). The spectra, which closely resemble similar data in ref. [7], clearly illustrate the formation of adsorbed CO species, on on-top (linear) CO_L (2000–2065 cm^{-1}) and on bridge or multifold sites (CO_M, 1790–1880 cm^{-1}). The spectra show a clear in-

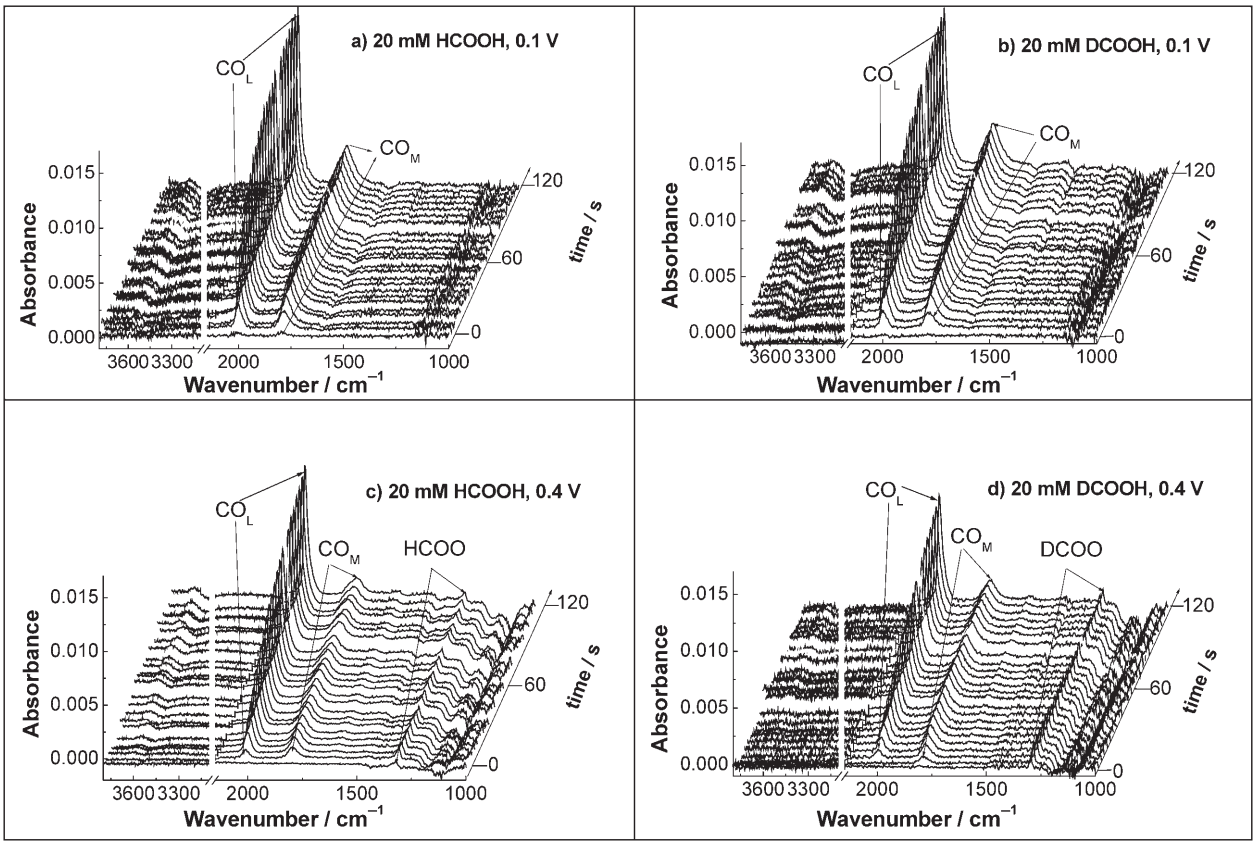

Figure 2. Sequences of in situ IR spectra recorded on a Pt film electrode after changing from a pure 0.5 M H_2SO_4 base electrolyte to a 0.5 M H_2SO_4 + 0.02 M HCOOH or DCOOH solution at a constant potential.

crease in intensity and peak frequency of the $CO_{L,M}$ band with time, reflecting an increasing CO_{ad} coverage. At potentials higher than 0.2 V, and at relatively low CO_{ad} coverages, we observe a characteristic peak at $\approx$1320 cm^{-1} [17,24] (1295 cm^{-1} for $DCOO_{ad}$[19]), which is related to adsorbed, bridge-bonded formates.[7]

Intensity–time profiles (Figure 3a: CO_L, Figure 3c: CO_M), evaluated as a function of time from the integrated IR intensities of the CO_L and CO_M species during formic acid adsorption/oxidation at different adsorption potentials between 0.1 and 0.5 V, show that the buildup of the CO adlayer is rapid in the potential range from 0.1 to 0.4 V and fastest at around 0.2 V. Furthermore, they reveal slower reaction kinetics for CO_{ad} formation during DCOOH adsorption (○) than during HCOOH adsorption (■).

The potential dependence during CO_{ad} formation can be described by a steady increase of the formic acid decomposition rate to CO_{ad}, with decreasing potential, plus an additional second process, which is most likely due to an increased surface blocking caused by adsorbed under-potential-deposited hydrogen atoms (H-upd), and leads to a reduction of the CO_{ad} formation at very cathodic potentials. This interpretation is supported also by the lower CO_{ad} saturation coverage at 0.1 V, which—in agreement with our own previous observations on Pt film electrodes and on carbon-supported catalysts—is only about $^2/_3$ of that at higher potentials (0.2–0.4 V).[7,25] Possibilities for the physical origin of the decrease in the CO_{ad} formation rate with the potential might be: 1) potential-dependent changes in the concentration or orientation of the likely precursors of the HCOOH molecules and the $HCOO^-$ anions near the interface, or 2) effects related to the polarity of the transition state for the CO_{ad} formation.

The differences between the CO_{ad} formation kinetics of HCOOH and DCOOH can be eliminated by plotting the CO_{ad} intensities on a normalized timescale, where the timescale for the deuterated reactant is divided by 1.9 (Figure 3b) to account for the slower buildup of CO_{ad} from the deuterated formic acid. The normalized intensity–time profiles are practically identical at all potentials, except at 0.5 V, where differences develop after about 500 s (adsorption time) and result in a lower steady-state CO_{ad} coverage for DCOOH than for HCOOH (Figure 4), which is explained by the onset of CO_{ad} oxidation, as will be discussed in detail later.

The observation of a constant factor of 1.9 between the rates of CO_{ad} formation from the HCOOH and DCOOH adsorption at potentials between 0.1 and 0.5 V provides clear proof that C–H bond breaking is indeed rate-limiting for the CO_{ad} formation by formic acid decomposition. In combination with recent results of highly surface-sensitive IR studies, which found no indication of a precursor for the CO_{ad} formation that is bound to the Pt surface via its carbon end,[7] this means[18–20] either that there is no stable adsorbed precursor for the CO_{ad} formation other than the weakly adsorbed $HCOOH_{ad}$ species or that CO_{ad} is formed by decomposition of $HCOO_{ad}$. The latter

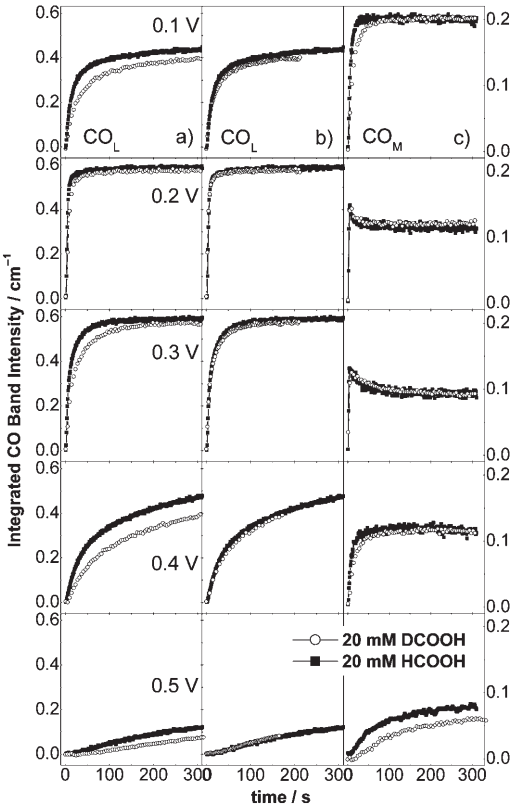

Figure 3. Integrated CO_L [column (a)] and CO_M [column (b)] band intensities obtained on a Pt film electrode as a function of time after changing from a 0.5 M H_2SO_4 solution to a 0.5 M H_2SO_4 + 0.02 M HCOOH (■) or DCOOH (○) solution at different constant potentials (0.1–0.5 V). Column (c): HCOOH- and DCOOH-based intensities as in the left columns but with the timescale for the DCOOH adsorption divided by 1.9.

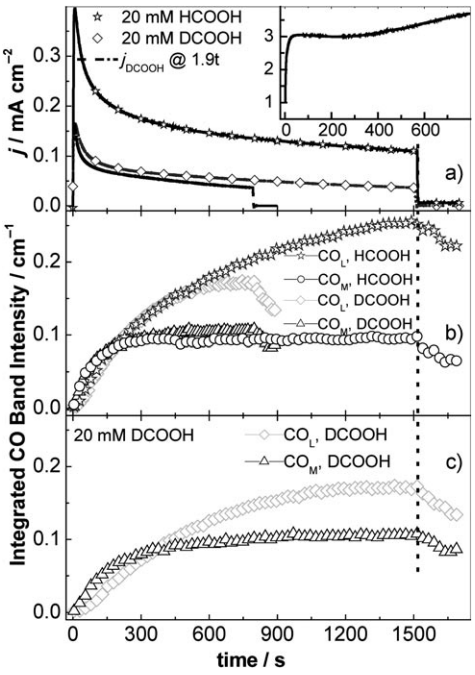

Figure 4. Faradaic current density (a) and integrated band intensity of $CO_{L,M}$ [(b), (c)], obtained as a function of time during long-term adsorption of 0.5 M H_2SO_4 + 0.02 M HCOOH or DCOOH on a Pt film electrode at 0.5 V and upon switching back to 0.5 M H_2SO_4 after 25 min while holding the electrode potential at 0.5 V. a) ☆: 20 mM HCOOH solution, ◇: 20 mM DCOOH solution, ——: 20 mM DCOOH solution with a normalized timescale (divided by 1.9); b) ☆; and ○: CO_L and CO_M from a 20 mM HCOOH solution, ◇ and △: CO_L and CO_M from a 20 mM DCOOH solution with a normalized timescale (divided by 1.9); c) ◇ and △: CO_L and CO_M from a 20 mM DCOOH solution. Inset in (a): KIE at 0.5 V as a function of time, as derived from the Faradaic current for HCOOH and DCOOH (time-normalized) oxidation.

appears, however, unlikely in view of recent theoretical results[26,27] and considering the opposite potential dependence of the two processes with enhanced CO_{ad} formation at lower potentials and increased formate adsorption at higher potentials. Finally, if there were an additional electrochemical reaction step occurring on a timescale comparable to that of the C–H bond breaking, this would result in a potential dependence of the measured KIE for the CO_{ad} formation.

The KIE of 1.9, measured for CO_{ad} formation, is significantly smaller than the value of about seven, which has been calculated for gas-phase C–H bond breaking at room temperature.[1] The difference in KIEs is explained by the different transition states in both situations. For the gas-phase reaction, the KIE was calculated assuming that the transition state is close to a complete dissociation, which leaves the difference in zero-point energies of the initial states as the difference in activation barrier for the two isotopomers. For the electrocatalytic reaction, we expect C–H bond breaking to go along with Pt–H (and presumably Pt–C) bond formation, which leaves a substantial difference in the zero-point energies of the transition state, thus reducing the difference in the activation energy for this process between the two different isotopomers and, consequently, also causing a reduction of the measured KIE.

At 0.5 V, and higher CO_{ad} coverage, we found an increasing deviation between the CO_{ad} buildup from HCOOH and DCOOH at longer adsorption times. Even when correcting for the KIE by using the normalized timescale for the DCOOH adsorption (assuming that the KIE for C–H bond breaking and thus the ratio between CO_{ad} formation in unlabeled and deuterated formic acid is the same as that observed at more cathodic potentials), we observe an increasing difference in the measured CO_{ad} formation rates after 500 s (Figure 4). This is attributed to CO_{ad} oxidation, which at this potential and at higher CO_{ad} coverages reaches rates comparable in magnitude to those of the CO_{ad} formation. Since the rate constant for CO_{ad} oxidation is independent of the hydrogen isotope in the original formic acid molecule, at $E \geq 0.5$ V the effective buildup of the CO adlayer from DCOOH should be more strongly affected by simultaneous CO_{ad} oxidation than that from HCOOH because of its lower CO_{ad} formation rate, in good agreement with observations.

The CO_{ad} oxidation rate at steady-state conditions (under the present reaction conditions) can be derived from the initial decay of the CO_L intensity after changing back to pure supporting electrolyte. Using the IR intensity–CO_{ad} coverage calibration given in ref. [7] leads to rates of 2.8×10^{-4} molecules site^{-1} s^{-1} (HCOOH) and 2.2×10^{-4} molecules site^{-1} s^{-1}

(DCOOH) at steady-state CO_{ad} coverages and at a potential of 0.5 V. The difference between the two rates results from the different steady-state CO_{ad} coverages for the two reactants. When analyzing the steady-state formic acid oxidation current (total Faradaic current in Figure 4a), the CO_{ad} oxidation rate is observed to be less than 0.1% of the total formic acid oxidation rate [0.29 molecules site^{-1} s^{-1} (HCOOH) and 0.08 molecules site^{-1} s^{-1} (DCOOH)] under these reaction conditions, confirming our previous statement that under most reaction conditions the *indirect pathway*, via CO_{ad} formation/CO_{ad} oxidation, is a minority pathway for formic acid oxidation.

Finally, we would like to introduce a normalized KIE for formic acid oxidation which describes the KIE in the Faradaic current measured under similar reaction conditions, that is, at the same potential and at similar adlayer composition and coverage. In the present case, this describes the KIE for the direct oxidation of formic acid to CO_2, which has been shown to be—by far—the dominant reaction pathway under these conditions on the bare Pt surface (the indirect pathway contributes at most by 0.1%). Its determination requires the additional knowledge of the CO_{ad} coverage during the reaction process, which, in these measurements, can be provided by the IR data. Faradaic currents for similar adlayer composition are obtained by using the normalized timescale for the DCOOH oxidation, in this case, by dividing the timescale by 1.9. The resulting time-normalized Faradaic currents for the DCOOH oxidation are then used to determine the normalized KIEs at different potentials by relating them to the HCOOH oxidation current at the same potential. Figure 1c shows the resulting evolution of the normalized KIEs at potentials between 0.3 and 0.5 V. At potentials <0.3 V this evaluation is not possible because of the too low currents, and even at 0.3 V it becomes problematic at longer reaction times.

For all three potentials, the normalized KIE quickly increases immediately after switching to the formic-acid-containing solution and reaches practically constant values (of about three) after 10–15 s. Hence, also the normalized KIE, measured for formic acid oxidation at comparable CO adlayer coverages, is higher than one, indicating that the C–H bond breaking is part of the rate-limiting step in the direct oxidation of formic acid to CO_2. The initially lower values, obtained within the first 10 s, are attributed to contributions from H-upd and anion displacement in the initial phase after the electrolyte exchange. The practically constant value of the normalized KIE with time reveals that it is independent of the CO_{ad} coverage, as long as this is identical for both isotopomers.

In general—also for the dominant direct pathway for formic acid oxidation—the C–H bond-breaking step is rate-limiting, but in this case, the rate-limiting step exhibits a KIE (of about three), which is significantly higher than that observed for the CO_{ad} formation (1.9). The above arguments point towards a transition state with a less stable C–H bond than that of the CO_{ad} formation, where isotope effects are less pronounced than in the initial state. In this case, the difference in the activation barrier is larger than that for a reaction involving a transition state with a more strongly bound H atom, which is the case for formic acid dehydration to CO_{ad}.

At potentials $E \geq 0.5$ V and longer adsorption times, where the CO_{ad} oxidation becomes significant under the present reaction conditions, the situation becomes more complex. Under these conditions, the measured KIE results from both the KIE in the dominant *direct pathway* and the difference in CO_{ad} coverage for both isotopomers, which remains even after correction for the different CO_{ad} formation rates. We again assume that HCOOH oxidation occurs only on CO_{ad}-free surface sites, which results, in the simplest case, in a linear decay of the formic acid oxidation rate with CO_{ad} coverage. Therefore, even after normalization of the adsorption timescale, the measured KIE does not reflect the KIE in the dominant reaction pathway, but represents a convolution of the KIE in the *direct pathway*, as a majority reaction pathway under these conditions,[7] and the different CO_{ad} coverages. Because of the lower steady-state CO_{ad} coverage during DCOOH adsorption/oxidation, the measured DCOOH oxidation rate should be higher than that expected for the (higher) CO_{ad} coverage obtained otherwise (in the absence of CO_{ad} oxidation), and therefore, the measured effective KIE obtained under steady-state conditions should be lower than the actual KIE in the rate-limiting step of the dominant pathway under these conditions. The experimental data show, however, an increase of the normalized KIE at longer reaction times. As measured in a number of similar experiments, the increase of the normalized KIE always starts when the CO_{ad} coverages resulting from the two reactants on a normalized timescale begin to deviate. Hence, it is clearly related to the buildup of the CO adlayer. Further investigations are underway to clarify this issue.

Finally, it is expected that at even higher potentials ($E \geq$ 0.75 V), where the steady-state CO_{ad} coverages are very low,[20] surface poisoning should play no significant role and the measured effective KIE should again be identical to the normalized KIE in the rate-limiting step of the dominant reaction pathway.

Conclusions

By studying the interaction of formic acid with a Pt film electrode by means of combined electrochemical and in situ IR measurements under controlled transport conditions, we show that: 1) the formation of CO_{ad} during the interaction of formic acid with Pt, which is formally described as dehydration of HCOOH, exhibits a potential-independent KIE for the C–H bond breaking ($k_{C-H}/k_{C-D} = 1.9$) in the potential range 0.1–0.5 V, and 2) the KIE in the dominant direct pathway (direct oxidation to CO_2) is significantly higher than that for CO_{ad} formation, reaching values of around three. These values indicate that in both pathways, the C–H bond-breaking step is rate-limiting and that the transition state in the latter pathway exhibits a weaker C–H (or Pt–H) bond than that for CO_{ad} formation. Finally, at more anodic potentials (here 0.5 V), the onset of the competing CO_{ad} oxidation, which is not affected by a KIE related to the HCOOH/DCOOH reactants, results in a change in the reaction characteristics, and thus in a change of the formic acid oxidation rate, by creating CO adlayers with different steady-state coverages for the two isotopomers, so that the

measured effective KIE can no longer be assigned to a single reaction step and its related KIE. The data demonstrate the potential of in situ spectroelectrochemical measurements for identifying and quantifying reaction-pathway-specific KIEs in a complex reaction network as basis for drawing conclusions on the nature of the rate-limiting steps and the transition states of the individual reaction pathways.

Acknowledgements

We gratefully acknowledge discussions with Prof. E. Spohr and Dr. sC. Hartnig. This work was supported by the Deutsche Forschungsgemeinschaft (project Be 1201/11-1) and by the Helmholtz Gemeinschaft (project VH-VI-139).

Keywords: electrochemistry · isotope effects · platinum · reaction kinetics · reaction mechanisms

[1] L. Melander, W. H. Saunders, *Reaction Rates of Isotopic Molecules*, Wiley, New York, **1980**.
[2] A. V. Tripkovic, K. D. Popovic, R. R. Adzic, *J. Chem. Phys.* **1991**, *88*, 1635.
[3] R. J. Madix, S. G. Telford, *Surf. Sci.* **1995**, *328*, L576.
[4] A. Wieckowski, *J. Electroanal. Chem.* **1977**, *78*, 229.
[5] R. M. van Effen, D. H. Evans, *J. Electroanal. Chem.* **1980**, *107*, 405.
[6] R. Holze, T. Luczak, M. Beltowska-Brzezinska, *Electrochim. Acta* **1994**, *39*, 485.
[7] Y.-X. Chen, M. Heinen, Z. Jusys, R. J. Behm, *Angew. Chem.* **2006**, *118*, 995; *Angew. Chem. Int. Ed.* **2006**, *45*, 981.
[8] A. Capon, R. Parsons, *J. Electroanal. Chem.* **1973**, *44*, 1.
[9] M. Watanabe, S. Motoo, *Denki Kagaku* **1973**, *41*, 190.
[10] J. Clavilier, R. Parsons, R. Durand, C. Lamy, J. M. Leger, *J. Electroanal. Chem.* **1981**, *124*, 321.
[11] B. Beden, A. Bewick, C. Lamy, *J. Electroanal. Chem.* **1983**, *148*, 147.
[12] S.-G. Sun, J. Clavilier, A. Bewick, *J. Electroanal. Chem.* **1988**, *240*, 147.
[13] D. S. Corrigan, M. J. Weaver, *J. Electroanal. Chem.* **1988**, *241*, 143.
[14] J. Willsau, J. Heitbaum, *Electrochim. Acta* **1986**, *31*, 943.
[15] R. Gomez, M. J. Weaver, *J. Electroanal. Chem.* **1997**, *435*, 205.
[16] G. Samjeské, A. Miki, S. Ye, M. Osawa, *J. Phys. Chem. B* **2006**, *110*, 16559.
[17] A. Miki, S. Ye, M. Osawa, *Chem. Commun.* **2002**, 1500.
[18] G. Samjeské, A. Miki, S. Ye, A. Yamakata, Y. Mukouyama, H. Okamoto, M. Osawa, *J. Phys. Chem. B* **2005**, *109*, 23509.
[19] G. Samjeské, M. Osawa, *Angew. Chem.* **2005**, *117*, 5840; *Angew. Chem. Int. Ed.* **2005**, *44*, 5694.
[20] Y.-X. Chen, S. Ye, M. Heinen, Z. Jusys, M. Osawa, R. J. Behm, *J. Phys. Chem. B* **2006**, *110*, 9534.
[21] Z. Jusys, *J. Electroanal. Chem.* **1994**, *375*, 257.
[22] M. V. ten Kortenaar, Z. I. Kolar, J. J. M. de Goeij, G. Frens, *J. Electrochem. Soc.* **2001**, *148*, E327.
[23] M. Heinen, Diploma Thesis, University of Ulm (Germany), **2004**.
[24] Y.-X. Chen, A. Miki, S. Ye, H. Sakai, M. Osawa, *J. Am. Chem. Soc.* **2003**, *125*, 3680.
[25] Z. Jusys, R. J. Behm, unpublished results.
[26] C. Hartnig, J. Grimminger, E. Spohr, unpublished results.
[27] C. Hartnig, E. Spohr, *Chem. Phys.* **2005**, *319*, 185.

Received: August 23, 2006
Published online on January 31, 2007

